World Applied Sciences Journal 24 (4): 457-462, 2013
ISSN 1818-4952

DOI: 10.5829/idosi.wasj.2013.24.04.2912

Dynamic Analysis of Tricept Parallel Manipulator with Principle of Virtual Work

Mir Amin Hosseini
Department of Mechanical Engineering,
Ayatollah Amoli Branch, Islamic Azad University, Amol, Iran

Submitted: Jun 1, 2013; **Accepted:** Jul 12, 2013; **Published:** Aug 18, 2013

Abstract: This paper investigates one of the complex degrees of freedom parallel manipulator, contains both rotational and orientational degrees of freedom, with machine tool application, known as Tricept PKM. Positioning and orienting rates via unique displacement in actuators, is one of the desired characteristics of robots with machine tools applications. The dynamic equations have been generated and solved for the optimum structure of Tricept PKM regard to have maximum dexterous work space by means of principle of virtual work. Hens, positioning and orienting rate will increase and the effects of operating delay will be neglectable.

Key word: Dynamic · Performance · Optimization · Parallel Manipulator · Virtual Work Method · Tricept

INTRODUCTION

Parallel manipulators have some advantages over their serial counterpart, such as low inertia, high stiffness, high load carrying capacity and high precision [1]. One of the famous parallel manipulator with both rotational and orientational degrees of freedom is Tricept. Tricept PKM is introduced by Neumann [2] and some desired characteristics led to be used in machining industries [3]. Pond and corretero [4] performed a comparison study among some similar parallel mechanism with the same degrees of freedom. They demonstrated the superiorities of Tricept with respect to the dexterity and workspace volume. Hosseini and daniali [5-7] introduced Weighted Factor method to normalizing Jacobian matrix and used for optimizing the dexterous workspace shape and size. They illustrated the optimized structure of Tricept completely differ from such as commonly used by some manufacturer. Generally, dynamic equation of parallel manipulator can be obtained by three different approaches. Newton-Euler method, Lagrangian formulation and principal of virtual work, are most well-known methods for obtaining dynamic equations. Wang and Gosselin [8] extracted dymaic equation of general stewart-gough parallel manipulator with principle of virtual work method. Here the dynamic equation is obtained by virtual work approach and some dynamic characteristics such as joint space velocities and forces are obtained for a random trajectory. Consequently, consuming power of actuators for the optimum structure regard to elder papers [5, 6], is illustrated. Conclusions led to estimating of elastic deformations and resulted uncertainty in positioning and orienting tasks.

Kinematics and Jacobian of Tricept PKM

Kinematic: Tricept robot, as depicted in Fig. 1, with two rotational and one translational dof was introduced by Neumann [2]. Siciliano [9] developed the kinematics and studied the manipulability of the Tricept. Pond and Corretero [4] formulate its square dimensionally homogeneous Jacobian matrices by furthering the method proposed by Kim and Ryu [10]. Architectural optimization of the Tricept and similar mechanisms was undertaken by Zhang and Gosselin [11].

The manipulator consists of base platform, moving platform, 3 active legs and one passive leg. Active legs are linear (prismatic) actuators which connect the base to the moving platform by universal (or spherical) and spherical joints. The passive leg consists of two parts; the upper part is a link with constant length which is connected to the moving platform by a spherical joint, while its lower part is a prismatic joint which is connected

Corresponding Author: Mir Amin Hosseini, Ayatollah amoli branch, Islamic Azad University, Amol , Iran.

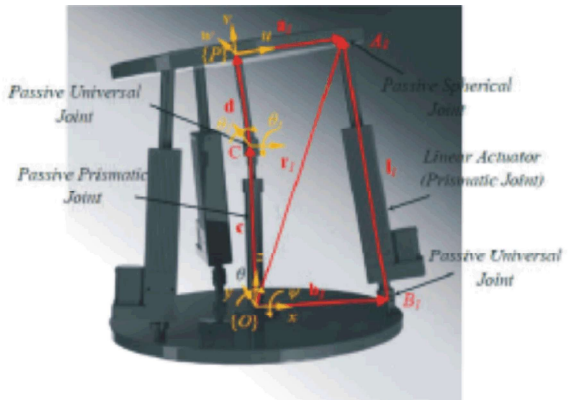

Fig. 1: Optimum Tricept PKM with maximum dexterous workspace

to the base and upper part by a passive universal joint. Moving and global frame, $\{P\ (uvw)\}$ and $\{O\ (xyz)\}$, are attached to the moving and base platform, respectively.

The geometric model of the i^{th} leg of Tricept is depicted in Fig. 1. The closure equation for this leg can be written as:

$$\mathbf{c} + \mathbf{R}(\mathbf{a}_i + \mathbf{d}) = b_i\mathbf{n}_{bi} + l_i\mathbf{n}_{li} \tag{1}$$

where **c** and **d** are the vectors from O to C and C to P, respectively. While **R** is rotation matrix carrying frame {P} into an orientation coincident with that of frame {O}; $\mathbf{a}_i$ is the position vector from P to A_i in frame $\{P\}$; $\mathbf{b}_i$ is the position vector of point B_i in the global frame. Moreover, $\mathbf{n}_{bi}$ and $\mathbf{n}_{li}$ are the unit vectors showing the directions of vectors $\mathbf{b}_i$ and $\mathbf{l}_i$, respectively.

Dot-multiplying both sides of Eq. (1) by $\mathbf{n}_{li}$, upon simplifications lead to:

$$\mathbf{c}^T\mathbf{n}_{li} + (\mathbf{R}\mathbf{a}_i + \mathbf{d})^T\mathbf{n}_{li} - \mathbf{b}_i\mathbf{n}_{bi}^T\mathbf{n}_{li} = l_i \tag{2}$$

Rewriting Eq. (2), for $i=1...3$, leads to three quadratic equations which can be solved either numerically or theoretically.

Jacobian Matrix: Taking the first time derivative of Eq. (1) yields:

$$\dot{c} + \omega_p \times \mathbf{R}\mathbf{a}_i + \mathbf{d} = \dot{l}_i\mathbf{n}_{li} + \omega_l \times l_i\mathbf{n}_{li} \tag{3}$$

where ω_p and ω_2 are the end-effector and limb angular velocity vectors. Dot-multiplying both sides of Eq. (3) by $\mathbf{n}_{li}$, upon simplifications lead to:

$$\mathbf{n}_{li}^T\dot{c} + \mathbf{n}_{li}^T\omega_p \times \mathbf{R}\mathbf{a}_i + \mathbf{d} = \dot{l}_i \tag{4}$$

Written Eq. (11), for $i=1...3$, yields:

$$\mathbf{A}\dot{\theta} = \mathbf{B}\mathbf{t} \tag{5}$$

where **t** is the three dimensional twist vector; $\dot{\theta}$ is the three dimensional actuator velocity vector; **A** and **B** are the Jacobian matrices, namely;

$$\mathbf{t} = \begin{bmatrix} \dot{c} & \dot{\psi} & \dot{\theta} \end{bmatrix}^T \tag{6}$$

$$\dot{\theta} = \begin{bmatrix} \dot{l}_1 & \dot{l}_2 & \dot{l}_3 \end{bmatrix}^T \tag{7}$$

$$\mathbf{B} = \begin{bmatrix} \mathbf{n}_{l1z} & (\mathbf{R}\mathbf{a}_1 + \mathbf{d}) \times \mathbf{n}_{l1}|_x & (\mathbf{R}\mathbf{a}_1 + \mathbf{d}) \times \mathbf{n}_{l1}|_y \\ \mathbf{n}_{l2z} & (\mathbf{R}\mathbf{a}_2 + \mathbf{d}) \times \mathbf{n}_{l2}|_x & (\mathbf{R}\mathbf{a}_2 + \mathbf{d}) \times \mathbf{n}_{l2}|_y \\ \mathbf{n}_{l3z} & (\mathbf{R}\mathbf{a}_3 + \mathbf{d}) \times \mathbf{n}_{l3}|_x & (\mathbf{R}\mathbf{a}_3 + \mathbf{d}) \times \mathbf{n}_{l3}|_y \end{bmatrix} \tag{8}$$

$$\mathbf{A} = \mathbf{I}_{3\times 3} \tag{9}$$

Moreover, the Jacobian matrix **J** is defined as:

$$\mathbf{J} \equiv \mathbf{B}^{-1}\mathbf{A} = \mathbf{B}^{-1} \tag{10}$$

Dynamic Equation: Here, dynamic equation of Tricept PKM is developed by principle of virtual work. On the assumption of frictionless contact between rigid bodies and time-invariant holonomic constraints, the principle of virtual works yields:

$$dw' + dw'' = 0 \tag{11}$$

where dw' is the elementary work of the actuating forces and dw'' is the elementary work of the inertial and gravitational forces, with null external forces and moments.

The first term can be computed

$$dw' = d\mathbf{q}_a^T\boldsymbol{\tau}_a \tag{12}$$

where $\boldsymbol{\tau}_a$ is the vector of joint actuating forces. The Jacobian has been used to express the elementary displacement in terms of task space variables.

$$d\mathbf{q}_a = \mathbf{J}^{-1}\,d\mathbf{x} \tag{13}$$

where $d\mathbf{x}$ is end-effector elementary displacement.

The second term of Eq. (11) can be computed by following equation:

$$dW = d\mathbf{q}_{n,p}^T \mathbf{f}_n + d\mathbf{q}_{n,o}^T \boldsymbol{\mu}_n + d\mathbf{q}_{m,p}^T \mathbf{f}_m + d\mathbf{q}_{m,o}^T \boldsymbol{\mu}_m + \sum_{i=1}^{3} (d\mathbf{q}_{S_i,p}^T \mathbf{t}_{S_i} + d\mathbf{q}_{S_i,o}^T \boldsymbol{\mu}_{S_i} + d\mathbf{q}_{N_i,p}^T \mathbf{t}_{N_i} + d\mathbf{q}_{N_i,o}^T \boldsymbol{\mu}_{N_i}) \quad (14)$$

where, $\mathbf{f}_n$ and $\boldsymbol{\mu}_n$ is exerted force and moment vector due to inertial and gravitational force and moment, on the lower part of middle link. Accordingly, ($\mathbf{f}_m$ and $\boldsymbol{\mu}_m$) dedicate to exerted force and moment on upper part of middle link. These terms, i.e., the exerted force and moments can be shown on screw by $\boldsymbol{\tau}_s$ and $\boldsymbol{\mu}_s$, respectively. Similarly they can be shown for nut connected parts by $\boldsymbol{\tau}_n$ and $\boldsymbol{\mu}_n$. Elementary rotational and translational displacement vector for associated elements, have been expressed by $d\mathbf{q}$ with o and p subscripts. Figure (1), shows the simple dynamic model of Tricept.

The central mass vector of each element is depicted in Fig. (2). With this regard, the parameters of Eq. 14, can be computed by follow:

$$\mathbf{f}_n = m_n(\ddot{\mathbf{P}}_n - \mathbf{g}_0) \quad (15)$$

$$\boldsymbol{\mu}_n = (r_n)\mathbf{f}_n \times \mathbf{z}_n \quad (16)$$

$$\mathbf{f}_m = m_m(\ddot{\mathbf{P}}_m - \mathbf{g}_0) \quad (17)$$

$$\mu_m = \mathbf{I}_m\dot{\omega}_m - \omega_m \times \mathbf{I}_m\omega_m - (r_m)\mathbf{f}_m \times \mathbf{z}_m \quad (18)$$

$$\mathbf{f}_{S_i} = m_S(\ddot{\mathbf{P}}_S - \mathbf{g}_0) \quad (19)$$

$$\mu_{S_i} = \mathbf{I}_S\dot{\omega}_i - \omega_i \times \mathbf{I}_S\omega_i + r_S\mathbf{f}_m \times \mathbf{z}_i \quad (20)$$

$$\mathbf{f}_{N_i} = m_N(\ddot{\mathbf{P}}_{N_i} - \mathbf{g}_0) \quad (21)$$

$$\boldsymbol{\mu}_{N_i} = \mathbf{I}_N\dot{\omega}_i - \omega_i \times \mathbf{I}_N\omega_i - (q_i - r_{N_i})\mathbf{f}_m \times \mathbf{z}_i \quad (22)$$

where, m_n, m_m, m_S and m_N are the upper and lower part of middle link and screw connected and nut connected part of the limbs masses. Moreover, $\mathbf{I}_m$, $\mathbf{I}_S$ and $\mathbf{I}_N$ are inertial tensors of the upper part of middle link, screw and nut connected parts, respectively. In addition, $\mathbf{g}_0$ is the vector of gravity acceleration. Related parameters can be computed as follow:

$$\ddot{\mathbf{P}}_n = \ddot{c}\mathbf{z} \quad (23)$$

$$\ddot{\mathbf{P}}_{S_i} = (l_{S_i})\dot{\omega}_i \times \mathbf{z}_i - (l_{S_i})\omega_i \times (\omega_i \times \mathbf{z}_i) \quad (24)$$

$$\ddot{\mathbf{P}}_{N_i} = \ddot{q}_i\mathbf{z}_i + 2\dot{q}\dot{\omega}_i \times \mathbf{z}_i + (l_{N_i})\dot{\omega}_i \times \mathbf{z}_i + (l_{N_i})\omega_i \times (\omega_i \times \mathbf{z}_i) \quad (25)$$

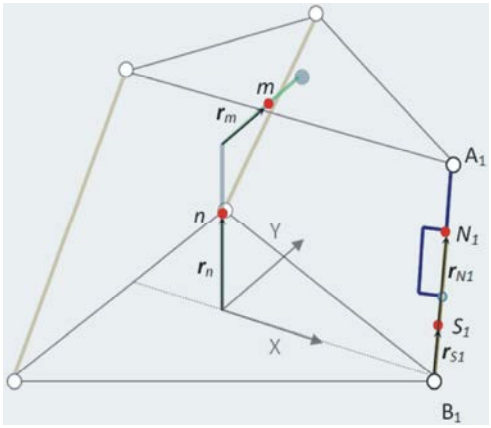

Fig. 2: Schematic of Tricept dynamic model

Equation (14) can be rewrite as follow:

$$dW = d\mathbf{x}^T ? \quad (26)$$

where,

$$? = \mathbf{J}_{n,p}^T \mathbf{f}_n + \mathbf{J}_{n,o}^T \boldsymbol{\mu}_n + \mathbf{J}_{m,p}^T \mathbf{f}_m + \mathbf{J}_{m,o}^T \boldsymbol{\mu}_m + \sum_{i=1}^{3} \mathbf{J}_{S_i,p}^T \mathbf{f}_{S_i} + \mathbf{J}_{S_i,o}^T \boldsymbol{\mu}_{S_i} + \mathbf{J}_{N_i,p}^T \mathbf{f}_{N_i} + \mathbf{J}_{N_i,o}^T \boldsymbol{\mu}_{N_i} \quad (27)$$

where, $\mathbf{J}_{n,p}$ ¡ $\mathbf{J}_{n,o}$ ¡ $\mathbf{J}_{m,p}$¡ $\mathbf{J}_{m,o}$ ¡ $\mathbf{J}_{si,p}$ ¡ $\mathbf{J}_{si,o}$ ¡ $\mathbf{J}_{Ni,p}$ and $\mathbf{J}_{Ni,o}$ are Jacobian matrices which transform end-effector translational and angular velocities into translational and angular velocities of each elements. They can be computed as follow:

$$\dot{\mathbf{P}}_n = \mathbf{J}_{n,p}\dot{\mathbf{x}} \quad (28)$$

where,

$$\mathbf{J}_{n,p} = \begin{bmatrix} \frac{\partial P_{n,1}}{\partial \psi} & \frac{\partial P_{n,1}}{\partial \theta} & \frac{\partial P_{n,1}}{\partial c} \\ \frac{\partial P_{n,2}}{\partial \psi} & \frac{\partial P_{n,2}}{\partial \theta} & \frac{\partial P_{n,2}}{\partial c} \\ \frac{\partial P_{n,3}}{\partial \psi} & \frac{\partial P_{n,3}}{\partial \theta} & \frac{\partial P_{n,3}}{\partial c} \end{bmatrix} = \begin{bmatrix} 0 & 0 & 0 \\ 0 & 0 & 0 \\ 0 & 0 & 1 \end{bmatrix} \quad (29)$$

Because of the lower part of middle link has not any rotational velocity:

$$\mathbf{J}_{n,o} = [0] \quad (30)$$

For the upper part of middle link:

$$\dot{\mathbf{P}}_m = \mathbf{J}_{m,p}\dot{\mathbf{x}} \tag{31}$$

where,

$$\dot{\mathbf{P}}_m = \begin{bmatrix} \frac{\partial P_{m,1}}{\partial \psi} & \frac{\partial P_{m,1}}{\partial \theta} & \frac{\partial P_{m,1}}{\partial c} & \frac{\partial \psi}{\partial t} \\ \frac{\partial P_{m,2}}{\partial \psi} & \frac{\partial P_{m,2}}{\partial \theta} & \frac{\partial P_{m,2}}{\partial c} & \frac{\partial \theta}{\partial t} \\ \frac{\partial P_{m,3}}{\partial \psi} & \frac{\partial P_{m,3}}{\partial \theta} & \frac{\partial P_{m,3}}{\partial c} & \frac{\partial c}{\partial t} \end{bmatrix}$$

$$\mathbf{J}_{m,p} = \begin{bmatrix} \frac{\partial P_{m,1}}{\partial \psi} & \frac{\partial P_{m,1}}{\partial \theta} & \frac{\partial P_{m,1}}{\partial c} \\ \frac{\partial P_{m,2}}{\partial \psi} & \frac{\partial P_{m,2}}{\partial \theta} & \frac{\partial P_{m,2}}{\partial c} \\ \frac{\partial P_{m,3}}{\partial \psi} & \frac{\partial P_{m,3}}{\partial \theta} & \frac{\partial P_{m,3}}{\partial c} \end{bmatrix} \tag{32}$$

or

$$\mathbf{J}_{m,p} = \begin{bmatrix} r_m S\psi S\theta & r_m C\psi C\theta & 0 \\ r_m C\psi & 0 & 0 \\ r_m C\theta S\psi & r_m S\theta C\psi & 1 \end{bmatrix} \tag{33}$$

For the angular velocities of end-effector and upper part of middle link, following equation exist.

$$\omega_m = \mathbf{J}_{m,o}\dot{\mathbf{x}} \tag{34}$$

where

$$\mathbf{J}_{m,o} = \begin{bmatrix} 1 & 0 & 0 \\ 0 & 1 & 0 \\ 0 & 0 & 0 \end{bmatrix} \tag{35}$$

And

$$\boldsymbol{\omega}_m = \begin{bmatrix} \dot{\theta}_1 \\ \dot{\theta}_2 C\theta_1 \\ \dot{\theta}_2 S\theta_1 \end{bmatrix} = \begin{bmatrix} \omega_x = \dot{\psi} \\ \omega_y = \dot{\theta} \\ \omega_z \end{bmatrix} \tag{36}$$

Due to pour translational velocity of screw connected part of the limbs, it led to:

$$\mathbf{J}_{S_i,p} = \begin{bmatrix} 0 \end{bmatrix} \tag{37}$$

Linear velocity vector of nut-connected part for the i^{th} limb is $\dot{q}_i\mathbf{z}_i$ in which $\mathbf{Z}_i$ is the direction of the limb in joint space coordinates, connected to the limb. Thus,

$$\mathbf{J}_{N_i,p} = \mathbf{z}_i\bar{\mathbf{j}}_i^T \tag{38}$$

where, $\bar{\mathbf{j}}_i^T$ is the i^{th} row of the inverse jacobian matrix, $\mathbf{J}^{-1}$.

Following equation exists for the angular transformer matrix for both nut and screw connected parts.

$$\mathbf{J}_{S_i,o} = \mathbf{J}_{N_i,o} \tag{39}$$

which can be rewritten as follow:

$$\mathbf{J}_{N_i,o} = \begin{bmatrix} S\psi_i S\theta_i & C\psi_i C\theta_i \\ C\psi_i & 0 \\ C\theta_i S\psi_i & S\theta_i C\psi_i \end{bmatrix} \mathbf{T}_i \tag{40}$$

In which T_i relates the end-effector velocity vector to the angular velocity vector of universal joints, as follow:

$$\begin{bmatrix} \dot{\psi}_i \\ \dot{\theta}_i C\psi_i \\ \dot{\theta}_i S\psi_i \end{bmatrix} = \mathbf{T}_i\dot{\mathbf{x}} \tag{41}$$

moreover, ϕ_i and θ_i are rotation around x and y axis of universal joints, which can be computed with respect to limb vector as follow:

$$S\psi_i = p_{iy}/q_i \tag{42}$$

$$C\psi_i S\theta_i = p_{iy}/q_i \tag{43}$$

Taking first time derivation and using chain rule $\mathbf{T}_i$ can be computed by Eq. (44).

$$\mathbf{T}_i = \begin{bmatrix} \frac{1}{q_i^2 C\psi_i}(q_i\mathbf{j}_{i,2}^T - p_{iy}\bar{\mathbf{j}}_i^T) \\ \frac{1}{C\theta_i C\psi_i}\left[q_i\mathbf{j}_{i,1}^T - \frac{p_{ix}\bar{\mathbf{j}}_i^T}{q_i^2}\right] \dot{\psi}_i S\psi_i S\theta_i \end{bmatrix} \tag{44}$$

where $\mathbf{j}_{i,k}^T$ is the k^{th} row of i^{th} limb jacobian matrix computed as follow:

$$\mathbf{J}_i = \begin{bmatrix} \frac{\partial P_{ix}}{\partial \psi} & \frac{\partial P_{ix}}{\partial \theta} & \frac{\partial P_{ix}}{\partial c} \\ \frac{\partial P_{iy}}{\partial \psi} & \frac{\partial P_{iy}}{\partial \theta} & \frac{\partial P_{iy}}{\partial c} \\ \frac{\partial P_{iz}}{\partial \psi} & \frac{\partial P_{iz}}{\partial \theta} & \frac{\partial P_{iz}}{\partial c} \end{bmatrix} \tag{45}$$

Table 1: Geometric parameters of Tricept robot

$d(mm)$	$r_b(mm)$	$r_a(mm)$
80.311	324.221	202.193

Table 2: Dynamic characteristics of assumed Tricept robot

$m_S(Kg)$	20
$m_m(Kg)$	700
$m_n(Kg)$	15
$I_N(Kg.m^2)$	$\begin{bmatrix} 0.046 & 0 & 0.002 \\ 0 & 0.045 & 0.004 \\ 0.002 & 0.004 & 0.001 \end{bmatrix}$
$I_S(Kg.m^2)$	$\begin{bmatrix} 0.298 & 0.204 & 0.152 \\ 0.204 & 0.557 & 0.077 \\ 0.152 & 0.077 & 0.491 \end{bmatrix}$
$I_m(Kg.m^2)$	$\begin{bmatrix} 0.828 & 0 & 0 \\ 0 & 0.828 & 0 \\ 0 & 0 & 1.614 \end{bmatrix}$

Trajectory Planning: Considering the optimum structure concluded from previous research work [6], cited in Table (1) and assumed dynamic performances cited in Table (2) a random trajectory generated with random amplitude and frequency.

Randomized trajectory for end-effector position is generated with following equations for two rotations and one elevation.

$$\psi(t) = A_{\psi}(t).Sin(\omega_{\psi}(t).t) \quad (46a)$$

$$\theta(t) = A_{\theta}(t).Sin(\omega_{\theta}(t).t) \quad (46b)$$

$$Z(t) = A_{Z}(t).Sin(\omega_{Z}(t).t) \quad (46c)$$

Considering 0.35 (rad) and 0.15 (m) for the maximum amplitude of angular and linear displacement and 0.8 Hz, for the maximum frequency, Figure 3, illustrates a random trajectory for end-effector displacement.

Taking first and second time derivation from generated data lead to end-effector velocity and acceleration diagram, as depicted in Figures 4 and 5.

Concluded diagram for determination of limbs length, velocities and accelerations are depicted in Figure 6(a-c).

Figure 7 shows the affected limbs forces and consumed power of actuators due to trajectory.

Figure 7, shows the maximum actuator force and power as 1430^{N} and 500^{w} power. With this regards it can be choose reliable actuator with required dynamic performances.

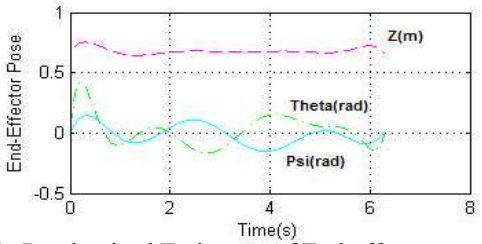

Fig. 3: Randomized Trajectory of End-effector

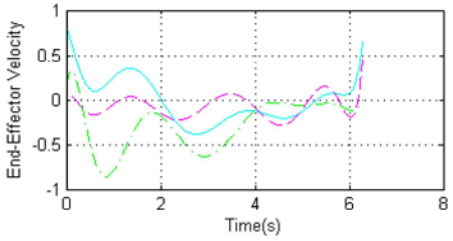

Fig. 4: Velocity of End-effector in Randomized Trajectory

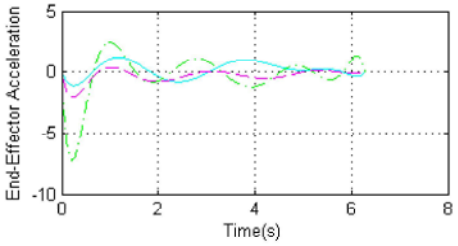

Fig. 5: Acceleration of End-effector in Randomized Trajectory

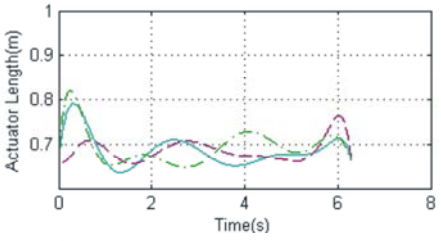

(a)

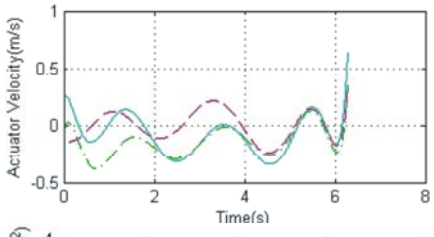

(b)

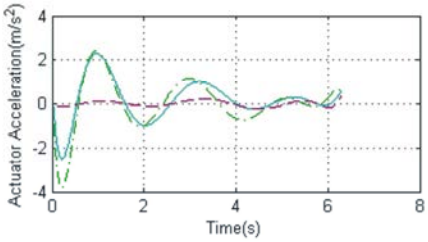

(c)

Fig. 6: Limbs displacements, velocities and acceleration due to randomized trajectory of EE

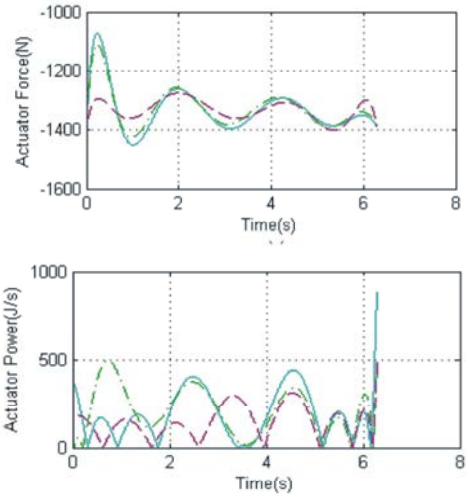

Fig. 7: Limbs forces and consumed power due to randomized trajectory of EE

CONCLUSION

One of the applicable parallel manipulator with complex degrees of freedom as Tricept, has been studied and dynamic equation for the optimum structure with maximum dexterous workspace has been released by principle of virtual work. As a case study, dynamic characteristics for a random trajectory generated via Matlab software.

REFERENCES

1. Merlet, J.P., 2006. Parallel Robots. Springer.
2. Neumann, K.E., 1988. US patent 4,732,525, Mar. 22.
3. www.pkmtricept.com.
4. Pond, G. and J.A. Carretero, 2007. Quantitative dexterous workspace comparison of parallel manipulators, Mechanism and Machine Theory, 42(10): 1388-1400.
5. Hosseini, M.A., H.R.M. Daniali and H.D Taghirad, 2011. Dexterous Workspace Optimization of a Tricept Parallel Manipulator, Advanced Robotics Journal, 25(1): 1697-1712.
6. Hosseini, M.A. and H.R.M. Daniali, 2011.Weighted Local Conditioning Index of Positioning and Orienting Parallel Manipulator**,** Scientia Iranica Journal, 18(1): 115-120.
7. Hosseini, M.A. and H.R.M. Daniali, 2011. Dexterous Workspace Shape and Size Optimization of a Tricept Parallel Manipulator, International Journal of Robotics, 2(1): 18-26.
8. Wang, J. and C.M. Gosselin, 1998. A new approach for the dynamic analysis of parallel manipulators, Multibody Syst. Dyn., 2: 317-334.
9. Siciliano, B., 1999. The Tricept robot: Inverse kinematics, manipulability analysis and closed-loop direct kinematics algorithm, Robotica, 17(4): 437-445.
10. Kim, S.G. and J. Ryu, 2003. New dimensionally homogeneous jacobian matrix formulation by three end-effector points for optimal design of parallel manipulators, IEEE Transactions on Robotics and Automation, 19(4): 731-737.
11. Gosselin, C.M., 1992. The optimum design of robotic manipulators using dexterity indices, Journal of Robotics and Autonomous Systems, 9(4): 213-226.